Optical band gap engineering of $(MgO)_x(ZnO)_{1-x}$ films deposited by sol-gel spin coating

S. TEMEL[a,*], M. NEBİ[b], D. PEKER[b]
[a]*Bilecik Seyh Edebali University, Central Research Laboratory, Bilecik, Turkey*
[b]*Eskisehir Osmangazi University, Physics Department, Eskisehir, Turkey*

The effects of magnesium oxide (MgO) doping on the characteristics of zinc oxide (ZnO) films have been investigated in this study. (MgO)x(ZnO)1-x thin films were deposited by sol-gel spin coating technique with different MgO concentrations. The structural, surface, optical and electrical properties of the films were characterized and the effects of doping on these properties were investigated. It was observed that the band gap of the (MgO)x(ZnO)1-x films can be adjusted by increasing the x values from 0 to 1. In addition structural, surface and electrical properties of the films were determined to vary according to the dopant concentration.

(Received April 21, 2017; accepted February 12, 2018)

Keywords: MgZnO thin films, Sol-gel preparation, Semiconductors, Band gap engineering

1. Introduction

ZnO thin films are one of the most important members of TCO materials and they are widely used in optoelectronic technology such as solar cells [1], photodetectors [2], liquid crystal displays (LCDs), organic light emitting diodes (OLEDs) and touch screen panels [3]. ZnO has advantages of low cost, non-toxicity and high chemical stability [4]. ZnO is a hexagonal wurtzite structure with an energy band gap of 3.3 eV [5]. However, there are limitations in the application of ZnO to the integrated optical devices because band gap of ZnO is not wide enough [6]. Optical band gap energy of ZnO thin films can be increased by doping with MgO [7]. Due to the ionic radius of Mg^{2+} and Zn^{2+} are similar [8], the substitution of Zn by Mg does not cause significant changes in lattice structure [9]. By doping ZnO with MgO the bang gap of MgZnO alloys can be tuned from 3.3 to 4 eV [10] according to dopant concentration. MgZnO films with wide optical band gap characteristic has several advantages for electro-optical application such as layer of light emitting diodes, buffer and TCO layers for thin film solar cells [6] Also, MgZnO is an ideal material for UV photodetectors because of its unique properties such as high radiation hardness and large tunable band gap range [11,12]. MgZnO thin films can be prepared by several methods like as Electron beam evaporation [13], RF Magnetron Sputtering [14], pulsed laser deposition [15], ultrasonic spray pyrolysis [16], electrospinning [17], mechanical milling [18] and sol-gel methods [19]. In this study, $(MgO)_x(ZnO)_{1-x}$ thin films were deposited by sol-gel spin coating technique with different MgO concentrations on glass substrates and the structural, surface, optical and electrical properties of the films were characterized.

2. Experimental details

$(MgO)_x(ZnO)_{1-x}$ thin films (x varies from 0 to 1) were deposited by sol-gel spin coating technique with different MgO concentrations on glass substrates. Zinc acetate dihydrate [$Zn(CH_3COO)_2.2H_2O$] for ZnO and magnesium chloride hexahydrate [$MgCl_2.6H_2O$] for MgO doping, were used as the starting precursors. 2-methoxyethanol and monoethanolamine (MEA) were used as solvent and stabilizer respectively and two different solutions were prepared for ZnO and MgO. The concentration of solutions was 0.5 M. After preparing these solutions, they were mixed together in different solution volume ratios to change the concentration x of MgO ranging from 0 to 1 with a step of 0.25. Finally five different solutions were obtained. These solutions are given in Table 1.

Table 1. Solutions and series of $(MgO)_x(ZnO)_{1-x}$ thin films

X	Solutions	Series
x= 0	ZnO	A
x= 0,25	$(MgO)_{0,25}(ZnO)_{0,75}$	B
x= 0,50	$(MgO)_{0,50}(ZnO)_{0,50}$	C
x= 0,75	$(MgO)_{0,75}(ZnO)_{0,25}$	D
x= 1	MgO	E

The solutions were spin coated onto glass substrates at a rotating speed of 3000 rpm for 30 seconds for each series. The coated thin films were dried at 150°C for 10 minutes. This process was repeated for 9 times to obtaining multilayer thin films. Finally, the obtained multilayer thin films were annealed at 500°C in air for 2 hours.

The crystal structures of the thin films were investigated by X-Ray Diffraction (XRD) measurements.

XRD measurements were performed by Panalytical Empyrean X-Ray diffractometer using CuK_α (λ=1.5405 Å) radiation in the 2θ range 30°-70° with a scanning speed of 2°/min. The surface morphology of the thin films was studied by FESEM (Zeiss Supra 40VP). Absorption studies in the UV-Vis. region were carried out at room temperature to determine the optical band gap of the thin films. UV-Vis spectroscopy measurements were analysed by Perkin Elmer Lambda 25 UV-Vis Spectrometer between 300-1100 nm wavelengths. Four-probe method was used to determine the electrical resistivity values of the thin films.

3. Results and discussion

In Fig. 1, XRD spectra of all series have been presented comparatively. All films are in a polycrystalline structure. In the A series, the XRD diffraction pattern of the pure ZnO has matched entirely with that of the hexagonal structured ZnO (ICDD: 98-003-1052). In B series, with the addition of 25% MgO, (002) peak of cubic MgO structure in a very small intensity in the XRD pattern has started to be observed. In the series C and D, the (111) and (022) peaks of the same structure have been formed, respectively, as well as the intensity of the (002) peak of the MgO structure. In the E series, the XRD diffraction pattern of the pure MgO has completely been converted to MgO (ICDD: 98-064-2712) in the cubic structure. In summary, as can be seen in Fig. 1, as the "x" value has increased in the $(MgO)_x(ZnO)_{1-x}$ films, that is to say, as the MgO content has increased, the number of MgO peaks in the XRD spectrum and the intensity of the peaks have also increased.

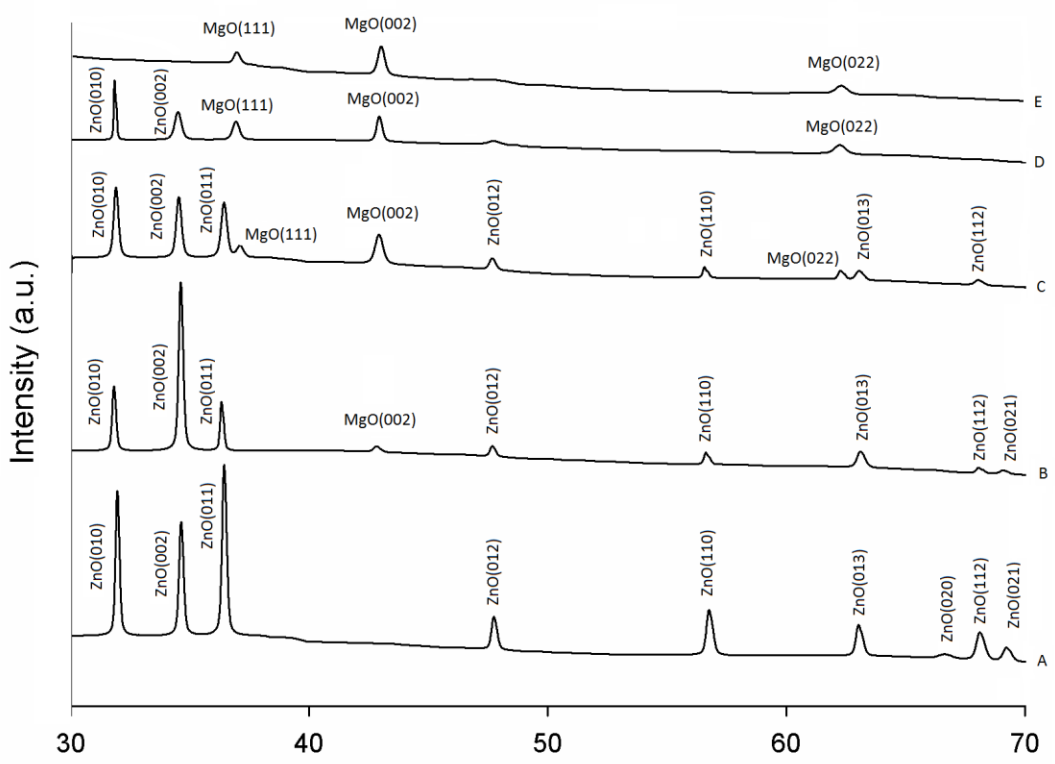

Fig. 1. XRD spectra of all series

In Fig. 2, FESEM images of all series are presented. When these images are examined, it is seen that the films have been coated homogeneously on the base. It is also understood that there haven't been any formations in the form of agglomerations and there haven't been any gaps on the surface, so that, the grains have better been connected to each other. In the A series, hexagonal ZnO structure has been seen. With the increase of the doping starting from the series B, it has appeared that the grains of MgO structure have increased on the surface towards the series C and D. In series E, the structure has completely been transformed into cubic MgO. Examining the FESEM images from series A to series E; it has been understood that the surface morphology changes depending on the MgO content ratio.

The band gap energies of the obtained films were determined according to the Tauc Method [20]. In Fig. 3, graphs of the variation of $(\alpha h\upsilon)^2$ versus $h\upsilon$ where the band gap energy of the films are determined are presented for all series comparatively. The point at which the linear part of the graph cuts the $h\upsilon$ axis gives the band gap energy value of the material. As can be seen from the graph, it has been observed that as the "x", which is doped in the $(MgO)_x(ZnO)_{1-x}$ films, value increases, in other words, as the MgO content increases, the band gap energy is widened. The increase in the value of the band gap energy

is due to the fact that the band gap energy of the MgO added to the structure is larger than the band gap energy of ZnO.

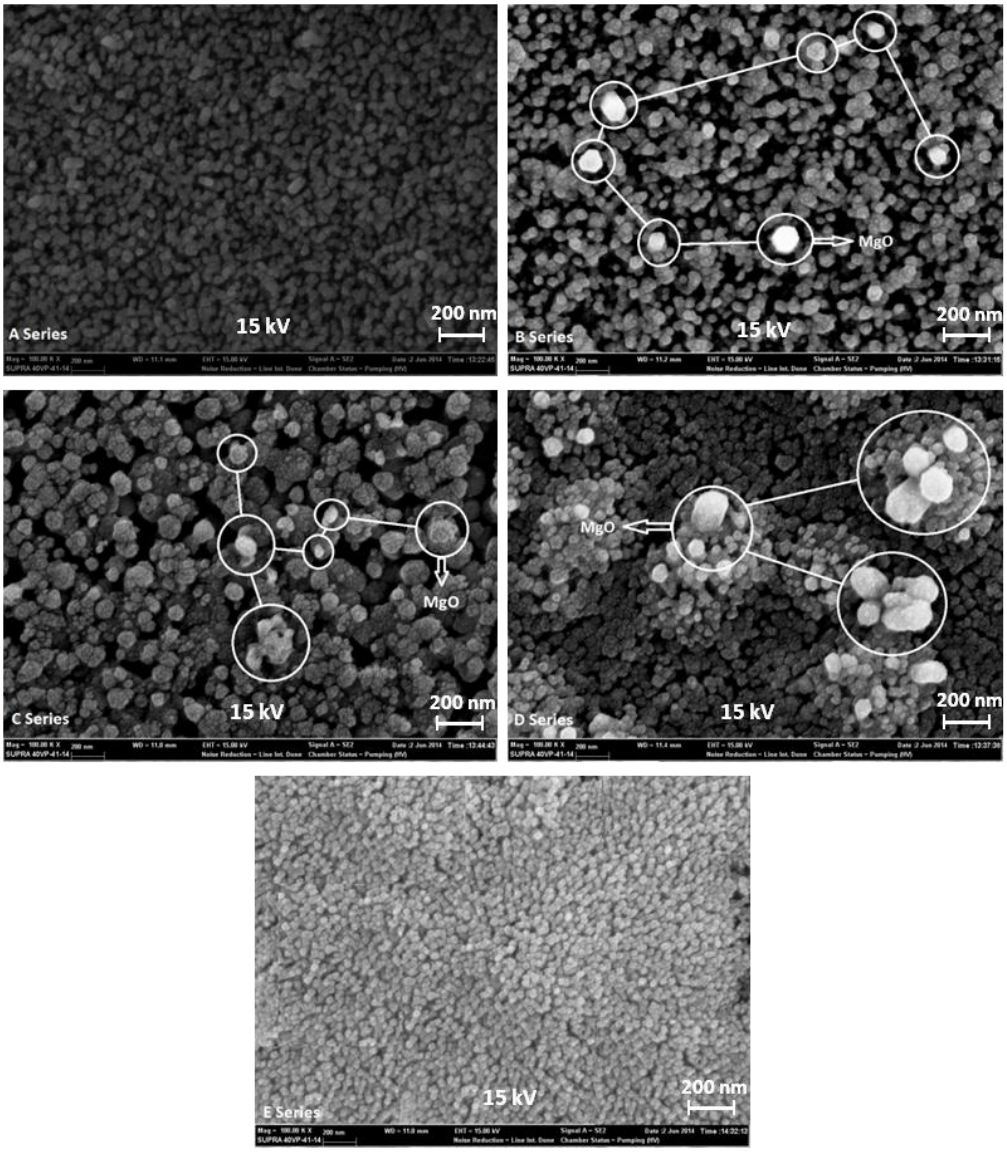

Fig. 2. FESEM images of all series

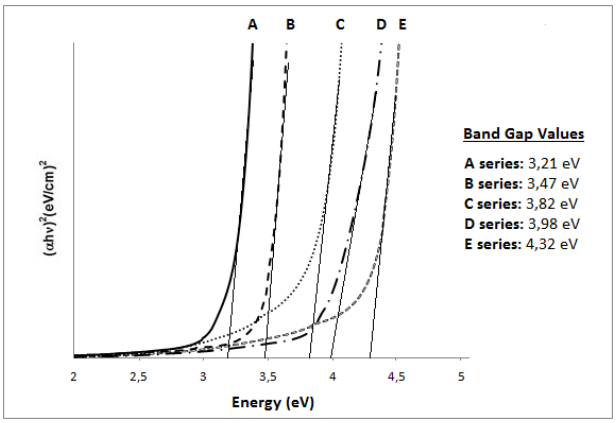

Fig. 3. The plots of $(\alpha h\upsilon)^2$ vs. $h\upsilon$ of all series and band gap values

Fig. 4 shows the electrical resistivity and conductivity changes of $(MgO)_x(ZnO)_{1-x}$ films measured by the four-point probe method. With the increase of the MgO addition, the electrical resistivity values of the films increase and the conductivity values decrease. When the XRD spectra of all the series are examined, it is understood that the MgO peaks which started to be observed from the series B and proliferate as the amount of additive increases, the hexagonal ZnO structure in the series A turns into the cubic MgO structure towards the E series. The change in this structure causes the increase of the resistivity value. In addition, the increase of the value of band gap energy depending on the concentration of the doping causes the increase of the resistivity value.

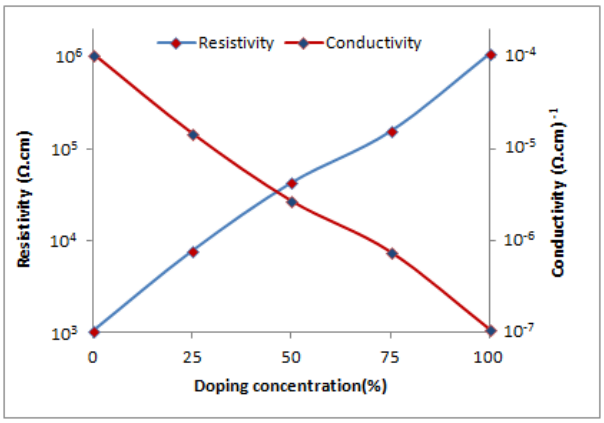

Fig. 4. Electrical resistivity and conductivity changes of $(MgO)_x(ZnO)_{1-x}$ films

4. Conclusion

As a result of these investigations, it has been determined that the structural, morphological, optical and electrical properties of MgO-doped ZnO films obtained vary depending on the doping concentration. The band gap of the $(MgO)_x(ZnO)_{1-x}$ films can be easily adjusted by increasing the additive concentration using the Sol-Gel Spin Coating method, an easy to apply and economical method. With this feature, doping of ZnO with MgO, which is frequently used in optoelectronic technology today, can help to extend the use of ZnO in optical filter applications, photonic devices operating in the UV region, and optoelectronic device applications such as LEDs.

References

[1] T. Minemoto, T. Negami, S. Nishiwaki, H. Takakura, Y. Hamakawa, Thin Solid Films **372**, 173 (2000).
[2] S. Liang, H. Sheng, Y. Liu, Z. Huo, Y. Lu, H. Shen, J. Cryst. Growth **225**, 110 (2001).
[3] S. W. Shin, I. Y. Kim, G. V. Kishor, Y. Y. Yoo, Y. B. Kim, J. Y. Heo, G. S. Heo, P. S. Patil, J. H. Kim, J. Y. Lee, J. Alloys Compd. **585**, 608 (2014).
[4] S. Gowrishankar, L. Balakrishnan, N. Gopalakrishnan, Ceram. Int. **40**, 2135 (2014).
[5] P. Bhattacharya, R. R. Das, R. S. Katiyar, Thin Solid Film **447**, 564 (2004).
[6] A. Kaushal, D. Kaur, Sol. Energy Mater. Sol. Cells **93**, 193 (2009).
[7] K. Huang, Z. Tang, L. Zhang, J. Yu, J. Lv, X. Liu, F. Liu, Appl. Surf. Sci. **258**, 3710 (2012)
[8] D. K. Hwang, M. C. Jeong, J. M. Myoung, Appl. Surf. Sci. **225**, 217 (2004).
[9] M. Caglar, J. Wu, K. Li, Y. Caglar, S. Ilican, D. Xue, Mater. Res. Bull. **45**, 284 (2010).
[10] M. Wang, E. J. Kim, S. Kim, J. S. Chung, I. K. Yoo, E. W. Shin, S. H. Hahn, C. Park, Thin Solid Films **516**, 1124 (2008).
[11] J. S. Shiau, S. Brahma, C. P. Liu, J. L. Huang, Thin Solid Films **620**, 170 (2016).
[12] C. Y. Zhao, X. H. Wang, J. Y. Zhang, Z. G. Ju, C. X. Shan, B. Yao, D. X. Zhao, D. Z. Shen, X. W. Fan, Thin Solid Films **519**, 1976 (2011).
[13] M. Ashraf, S. M. J. Akhtar, A. Qayyum, Mater. Sci. Semicond. Process **15**, 251 (2012).
[14] Y. Zhao, D. Jiang, R. Liu, Q. Duan, C. Tian, L. Sun, S. Gao, J. Qin, Q. Liang, J. Zhao, Solid State Electron. **111**, 223 (2015).
[15] J. Y. Cho, S. W. Shin, Y. Bin Kwon, H.-K. Lee, K. U. Sim, H. S. Kim, J.-H. Moon, J. H. Kim, Thin Solid Films **519**, 4282 (2011).
[16] X. Zhang, X. M. Li, T. L. Chen, J. M. Bian, C. Y. Zhang, Thin Solid Films **492**, 248 (2005).
[17] S. S. Cetin, I. Uslu, A. Aytimur, S. Ozcelik, Ceram. Int. **38**, 4201 (2012).
[18] S. Suwanboon, P. Amornpitoksuk, Procedia Engineering **32**, 821 (2012).
[19] J. Y. Moon, H. Kim, H. S. Lee, Thin Solid Films **546**, 461 (2013).
[20] J. Tauc, Amorphous and liquid semiconductors, New York: Plenum, (1976).

*Corresponding author: sinan.temel@bilecik.edu.tr